

2D and 3D stem cell models of primate cortical development

identify species-specific differences in progenitor behavior

contributing to brain size

Running title: Species progenitor cell differences and brain size

Tomoki Otani¹, Maria C. Marchetto², Fred H. Gage², Benjamin D. Simons³ and Frederick J. Livesey^{1*}

¹Gurdon Institute and Department of Biochemistry, University of Cambridge, Tennis Court Road, Cambridge CB2 1QN

²The Salk Institute, Laboratory of Genetics, North Torrey Pines Road, La Jolla, CA.

³Gurdon Institute, Cambridge Stem Cell Institute and Department of Physics, University of Cambridge, Cambridge

*Author for correspondence:

Gurdon Institute, University of Cambridge, Tennis Court Road, Cambridge, CB2 1QN, UK.

Email: rick@gurdon.cam.ac.uk

SUMMARY

Variation in cerebral cortex size and complexity is thought to contribute to differences in cognitive ability between humans and other animals. Here we compare cortical progenitor cell output in humans and three non-human primates using directed differentiation of pluripotent stem cells (PSCs) in adherent two-dimensional (2D) and organoid three-dimensional (3D) culture systems. Clonal lineage analysis showed that primate cortical progenitors proliferate for a protracted period of time during which they generate early-born neurons, in contrast to rodents where this expansion phase largely ceases before neurogenesis begins. The extent of this additional cortical progenitor expansion differs among primates, leading to differences in the number of neurons generated by each progenitor cell. We found that this mechanism for controlling cortical size is regulated cell-autonomously in culture, suggesting that primate cerebral cortex size is regulated at least in part at the level of individual cortical progenitor cell clonal output.

INTRODUCTION

The cerebral cortex is the integrative and executive centre of the mammalian central nervous system, making up over three-quarters of the human brain (Mountcastle et al., 1998). An increase in neuronal number, and thus cerebral cortex size, is thought to provide a template for more complex neural architectures, contributing to differences in cognitive abilities between humans and other primates (Geschwind and Rakic, 2013; Herculano-Houzel, 2012). The developmental mechanisms that generate differences in neuronal number and diversity, and thus cerebral cortex size in humans, other primates and mammals in general, are currently poorly understood.

During embryonic development, all excitatory cortical projection neurons are generated directly or indirectly from neuroepithelial progenitor cells of the cortical ventricular zone (VZ) (Rakic, 2000). A common feature of cerebral cortex development in all mammals is that multipotent cortical progenitor cells produce multicellular clones of neurons over developmental time, generating different classes of cortical projection neurons and then glial cells in fixed temporal order (Kornack and Rakic, 1995; McConnell, 1988; 1992; Walsh and Cepko, 1988). Neuroepithelial cells are the founder progenitor cell population in the cerebral cortex, giving rise to neurogenic radial glial cells that generate all of the excitatory neurons of the cerebral cortex, either directly or indirectly (Florio and Huttner, 2014; Mountcastle et al., 1998). Radial glial cells can self renew (proliferate), directly generate post-mitotic neurons or produce two different types of neurogenic progenitor cells: intermediate/basal progenitor cells (IPCs) and outer radial glial cells (oRGs) (Florio and Huttner, 2014; Geschwind and Rakic, 2013; Herculano-Houzel, 2012; LaMonica et

al., 2012). Both basal progenitor cells and oRGs can also self renew or generate neurons, with some evidence that IPCs have limited proliferative capacity (Gertz et al., 2014; Rakic, 2000).

Although several different processes have been proposed to contribute to increased neuronal numbers in the primate cortex (Herculano-Houzel, 2009), research has focused on two primary mechanisms: an increase in the number of founder neuroepithelial cells, driven by increased proliferation of neuroepithelial cells before entering the neurogenic period of cortical development (Florio and Huttner, 2014; Geschwind and Rakic, 2013); and an increase in the number of oRG cells, as found in primates (Hansen et al., 2010). The latter in turn amplify the output of radial glial cells (for a recent review, see (Dehay et al., 2015)). The radial unit hypothesis proposes that an increase in the number of founder neuroepithelial cells is the basis for the increase in cortical size in humans compared with other primates (Geschwind and Rakic, 2013; Rakic, 2000). The identification of oRGs in primates and other mammals has led to a modification of the radial unit hypothesis to suggest that the addition of oRGs effectively increases the progenitor population and thus is a major contributor to primate cortical expansion (Fietz et al., 2010; Hansen et al., 2010; Smart et al., 2002).

Current models for the cellular mechanisms that generate the increased numbers of neurons found in the primate cerebral cortex rely on extrapolating from a large body of work on rodent, primarily mouse, cortical neurogenesis. However, the cortex of humans and other primates appears to follow different scaling rules than that of other mammals,

including mouse, in terms of the relationship between cortical volume and cell number and overall body size (Azevedo et al., 2009). We and others have developed human stem cell systems to study cerebral cortex neurogenesis *in vitro* (Espuny-Camacho et al., 2013; Mariani et al., 2012; Shi et al., 2012a), finding that directed differentiation of human pluripotent stem cells (PSCs) to cerebral cortex progenitor cells robustly replays the temporal order of cortical neurogenesis, including the production of the diversity of progenitor cell types found *in vivo* (Shi et al., 2012a).

In this study, we extended the use of stem cell systems to compare human, macaque and chimpanzee cortical neurogenesis to understand the developmental mechanisms regulating increased cortical size in different primates. We find that there are several important differences in cerebral cortex progenitor cell biology between rodents and primates, and between humans and non-human primates, which contribute to the marked differences in neuronal number among the different species. Together, these findings constitute multiple new insights into the biology of generating large brains in relatively slowly developing mammals, including primates.

RESULTS

Replication of species-appropriate developmental timing of cortical neurogenesis *in vitro* from PSCs of multiple primate species

We used stem cell systems to analyse the relationships between progenitor cell proliferation dynamics, clonal output, neuronal number and cortical size in four species of primate with differing brain sizes. We compared cortical neurogenesis among humans, the chimpanzee *Pan troglodytes* (Marchetto et al., 2013), a great ape with less than half the number of cortical neurons of humans (Herculano-Houzel et al., 2007), and in two species of Old World monkey, the crab-eating macaque, *Macaca fascicularis*, and the southern pig-tailed macaque, *Macaca nemestrina*, both of which have cerebral cortices with approximately one-tenth the numbers of neurons as humans (Herculano-Houzel et al., 2007).

We applied our previously described methods for directed differentiation of human PSCs to cerebral cortex to generate cortical progenitor cells of each species (Shi et al., 2012a; 2012b). Following neural induction, neuroepithelial cells generated the different populations of progenitor cells found in the mammalian cerebral cortex, including radial glial cells (RGCs) and IPCs (Fig. 1A, B). These progenitor cells were arranged in characteristic rosette structures, composed of polarized RGCs with their apical surfaces concentrated at the rosette centre, and IPCs located at the basal/peripheral region of the rosette (Shi et al., 2012a). Neuroepithelial rosettes were confirmed as dorsal pallial in regional identity by positive and negative expression of region-specific transcription factors (Fig. 1C).

To further investigate whether *in vitro* directed differentiation accurately captured *in vivo* progenitor cell diversity, we labeled individual cortical progenitor cells by lentiviral infection with GFP expression constructs to observe progenitor cell morphologies and cell division types. Bipolar progenitor cells, with characteristic ventricular RGC (vRG) morphology, were found within rosettes, whereas unipolar progenitor cells, with typical oRG morphologies, were found at the periphery of rosettes, (Supplementary Fig. 1A). Live imaging demonstrated that the different progenitor cell types underwent characteristic, cell type-specific mitotic cell body movements (Gertz et al., 2014; Ostrem et al., 2014): vRGs displayed interkinetic nuclear migration, whereas oRGs underwent mitotic somal translocation (Supplementary Fig. 1B, C).

Excitatory, glutamatergic neurons destined for each cortical layer are produced in a fixed temporal order during development, beginning with layer 6 (TBR1+) neurons, followed by neurons of each of the other five layers (Fig. 1D)(Mountcastle et al., 1998). The fixed order of cortical neuron production was preserved *in vitro* for all non-human primates (Fig. 1E), as we previously reported for humans (Shi et al., 2012a). Furthermore, the timing of generation of different cell types followed species-specific timing *in vitro*. All species generated layer 6 neurons at approximately the same stage *in vitro* (20 days after initiating neural induction from PSCs, referred to as d20), as observed *in vivo* (Workman et al., 2013).

Both human and chimpanzee cortical progenitor cells switched from deep to upper layer neurogenesis 40-50 days later, as indicated by the appearance of SATB2+ layer 2-4 neurons (Fig. 1E, F). This finding is consistent with the approximately 45-day interval between layer 6 and layer 4 genesis in the developing human embryo (Workman et al., 2013). In contrast, cortical progenitor cells from both macaque species switched to upper layer neuron production less than 20 days after deep layer neurogenesis, reflecting the reported 19-day interval between these developmental events *in vivo* (Workman et al., 2013). The difference in the timing of the differentiation of upper layer neurons between human, chimpanzee and macaques was further confirmed by analyzing the time course of expression of additional genes specifically expressed by neurons of layers 2-4 and 5-6 (*CTIP2*, layer 5 and 6; *RORB*, *KCNIP2*, *MDGA1* for layers 2-4; Fig. 1G).

Timing of cortical neurogenesis is independent of neuronal lamination and 3D organisation

We observed conservation of development timing of cortical neurogenesis using differentiation of adherent, polarized neuroepithelial rosettes. Under these culture conditions, cortical neurons are highly migratory and form dense cultures that are 100-200 μm thick (Kirwan et al., 2015). However, they do not form the ordered layers of projection neurons (laminae) found in the cortex *in vivo* (Kirwan et al., 2015). To investigate whether lamination altered development timing, we also studied the timing of differentiation of deep and upper layer cortical neurons in non-adherent, 3D cortical organoids that underwent some degree of lamination and resembled the *in vivo* cortex in

terms of the spatial relationships of the progenitor cell populations and the post-migratory neurons (Fig. 2A) (Kadoshima et al., 2013).

As in the non-laminating rosette system, we found that deep layer TBR1+ cortical neurons appeared first in each species (Fig. 2B), followed by SATB2+ upper layer neurons that migrated to the basal/outer surface (Fig. 2B and 2C). The timing of the interval between the appearance of deep and upper layer neurons in organoids was in line with that which we observed in the rosette system for humans, chimpanzees and macaques. Upper layer neurons were present in large numbers in macaque cortical organoids at d60, at which stage there were few upper layer, SATB2+ neurons in the human and chimpanzee organoids (Fig. 1B). At d80 in human and chimpanzee organoids there was a substantial population of SATB2+/TBR1- upper layer neurons that had migrated and began laminating near the outer/pial surface (Fig. 2B and 2C).

Functional maturation of primate cortical neurons demonstrates species-specific timing

We previously found that *in vitro*-derived human cortical neurons undergo electrophysiological maturation over a prolonged period, compared with rodents, as also occurs *in vivo* (Shi et al., 2012a). To investigate the developmental maturation of non-human primate cortical neurons, we performed single neuron patch-clamp recordings of human, chimpanzee and macaque neurons. Miniature excitatory post-synaptic currents were detected in neurons of each primate species, confirming that neurons in each case efficiently formed functional synapses (Fig. 3A).

Using action potential firing in response to current injection as a measure of neuronal maturity, we found that macaque neurons of both species matured more quickly than both human and chimpanzee (Fig. 3B). Analysing neuronal maturity at a range of developmental stages (d30-d70), we found that functionally mature neurons were present at an earlier stage and at higher frequency in macaques than in humans and chimpanzees (Fig. 3B). Therefore, consistent with differential developmental timings of neurogenesis for each primate species, the maturation of cortical neurons also reflected species-specific timing *in vitro*, with humans and chimpanzees demonstrating similar rates of neuronal maturation.

Clonal analysis reveals marked differences between human and macaque cortical progenitor cell dynamics over developmental time

The number of neurons generated by a cortical progenitor cell (clone size) is a major contributor to total cell number and thus overall size of the cerebral cortex. Clonal lineage analysis of *in vitro*-derived cortical progenitor cells enables detailed comparisons of cortical progenitor cell dynamics and clonal outputs between species. Given the marked differences in cortex size, cortical neuronal number and developmental timing between humans and macaques, we focused our analyses on comparing cortical progenitor cell outputs between those species. Single cell clonal analysis was carried out using GFP-expressing, replication-incompetent lentiviral labeling of individual progenitor cells at 10-day intervals (d20, 30 or 40 post-cortical induction; Fig. 4A, B).

Clones (comprised of two cells or more and therefore rooted in labeled progenitor cells) were collected and analysed 2, 6 and 10 days after labeling, generating data on clone size distributions for progenitor cells labeled at each developmental stage (d20, d30 and d40). Clonal analyses were carried out in multiple pluripotent stem cell lines in humans [embryonic stem (ES) and induced pluripotent stem (iPS) cells] and macaque (ES cells). The accuracy of our assignment of clone membership was tested by two methods. First, we tested whether our sparse labeling method, using low titre viral infection, led to more than one infection event in close proximity. Mixing mCherry and GFP-expressing viruses before infection and clone labeling demonstrated that the occurrence of mixed GFP/mCherry labeled clones was extremely rare (Supplementary Fig. 2A). Second, using nearest neighbor analysis, we analysed the spatial distribution of labeled cells and found that it was highly improbable, assuming a starting random distribution of single labeled cells, that clones were merged separate infection events, as a consequence of clonal expansion and/or migration (Supplementary Information 1; Supplementary Fig. 2B, C).

In each cohort of progenitor cells labeled at the different time points (d20, d30 or d40) in both species, we observed a steady increase in average clone size over the 10-day period after labeling (Fig. 4C). For humans, we observed that the increase in overall clone size over the 10 days after labeling was very similar in cortical progenitor cells labeled at each developmental age (Fig. 4C). In contrast, clone size distributions in macaques changed between d20 and d40. The clone size distributions from the macaque d20 time course were similar to those in humans. However, clones generated by progenitor cells labeled at d30 and d40 did not expand to the same degree as those at d20 (Fig. 4C).

Importantly, we saw little variation in proliferative behaviours of progenitor cells derived from different cell lines of the same species (Supplementary Fig. 2D). Reflecting the inter-species difference in clonal expansion, we found that the average size of clones at each time point diverged between humans and macaques later in development, with older macaque cortical progenitor cells making significantly smaller clones on average than human progenitor cells (Fig. 4D). Therefore, macaque progenitor cells underwent a change in proliferative behavior over the d20-d40 period, leading to a reduction in total clone size. In contrast, human progenitor cells did not alter their proliferative behaviour and clonal outputs over this time period.

Differences in clone growth between macaque and human are reflected in differences in progenitor cell proliferative behaviours

Clonal lineage data suggest that macaque progenitor cells undergo a time-dependent change in their proliferative behaviour, which would reduce the numbers of progenitor cells per clone at later stages of development. We investigated this finding further by analyzing clone composition in terms of neurons and progenitor cell numbers. We found that the average number of progenitor cells per clone (as assessed by Ki67 expression) increased over the 10 days after labeling at all developmental stages in humans (Fig. 5A). In macaques, the number of progenitor cells plateaued at an average of around just one progenitor cell per clone at later stages of development (Fig. 5A), consistent with the reduction in clonal output by later stage macaque progenitor cells. This finding suggested that human and macaque progenitor cells had distinct proliferative behaviours at later

developmental ages, with human progenitor cells continuing to expand their population for a longer period than macaque.

The observed changes in proliferative behaviour ought to be underpinned by differences in progenitor cell division types. To gain further insight into the division patterns of progenitor cells, we judged each clone as either persisting or exited, depending on whether the clone contained at least one progenitor cell (Fig. 5B, C). Analysis of the size distribution of persisting clones, representing the population of progenitor cells containing at least one Ki67+ cell, revealed an approximately exponential increase in average clone size for human progenitor cells labeled at d40, compared to a linear-like increase in macaque (Fig. 5B). This finding suggested that a higher proportion of human progenitor cells were dividing symmetrically to generate additional progenitor cells, whereas macaque progenitor cells followed a more asymmetric or neurogenic division pattern. We found that approximately 15% (human) and 60% (macaque) of progenitor cells had exited proliferation 10 days after labeling (Fig. 5C), implying that the majority of macaque progenitors were terminally differentiating at this stage.

Clonal analysis suggests that macaque progenitor cells cease their progenitor expansion phase earlier in development than human. To test this, we applied a computational model informed by the findings of a recent *in vivo* genetic labeling study of cortical neurogenesis in mouse that showed that cortical progenitor cells transit sequentially through a symmetrical proliferative phase to a neurogenic phase in which cells make a

sequence of asymmetric cell divisions giving rise to IPCs, the latter having variable but limited proliferative potential (Gao et al., 2014).

Using experimentally measured parameters of apoptosis (Supplementary Fig.3A, B) and cell cycle length (Supplementary Fig. 4), we found that such hypotheses, and hence the model (Supplementary Information 2), could explain the differences in clonal behaviours between human and macaque, including the distribution of clone size and composition, as well as the frequency of terminally differentiated clones at the latest (10 day) time point (Fig. 5D and Supplementary Fig. 3C,D). Therefore, the clonal analysis data and the computational model together demonstrated that human cortical progenitor cells had an extended period (d20-d50) during which production of cortical neurons was balanced with production of additional progenitor cells. This finding is in contrast with macaque progenitor cells, which switched much earlier (at around 35) to a more neurogenic programme at the expense of production of progenitor cells.

Testing predictions of progenitor cell proliferative behaviours during human and macaque cortical development

To assess the validity of the model and the findings of the clonal analyses, we carried out two different experiments to analyse the proliferative capacity and division types of human and macaque progenitor cells. First, we designed a strategy to assess the proliferative capacity of human and macaque cortical progenitor cells between d40 and d46. This is the critical time window that we identified during which human and macaque progenitor cell division types diverge in their proliferative potential. We made use of an

EdU/BrdU double-labeling strategy to first label all cycling progenitor cells and their progeny over a 5-day interval with BrdU, followed by a final 24-hour EdU pulse to identify the fraction of that population that were still cycling (i.e., were cycling progenitor cells; Fig. 6A).

We found that some 31.2% (macaque) and 48.2% (human) of the progeny of d40 progenitor cells entered into cell cycle between day 5 and 6 after initial labeling (Fig. 6B). These numbers compare favourably with the model that, according to the clonal fits, predicted that some 29% (macaque) and 44% (human) of the progeny would have re-entered into cycle over this time interval (Supplementary Information 2).

In separate experiments, we used live time-lapse imaging to visualize progenitor cell division types in both species over 7 days (168 hours from d38 of post-cortical induction) to directly measure the proportion of different progenitor cell division types (Fig. 6C). In all, 21 human lineages (from two separate experiments) and 22 macaque lineages (from two separate experiments) were analysed (Fig. 6D). A wide range of cell cycle lengths was observed in each species, between 12 and over 100 hours, with a mean cell cycle length in macaque of 36.2 hours compared with 46.5 hours in human (Fig. 6E). These averages from direct observations were consistent with the Pax6-positive population cell cycle length averages measured by cumulative EdU labeling of 47.1 hours in human and 37.7 hours in macaque.

Progenitor cell divisions were designated as proliferative (generating two progenitor cells), neurogenic (generating one progenitor and one neuron) or terminal (generating two neurons), depending on the outcome of the subsequent round of division. Divisions were only defined as neurogenic if one of the two cells did not re-enter cell cycle during the entire imaging period (Fig. 6C). The majority of human progenitor cell divisions were proliferative (56.3% of 112 divisions; Fig. 6F), compared with 29.4% of macaque divisions (of a total of 119; Fig. 6F). Conversely, 43.7% of macaque divisions were terminal (generating two post-mitotic cells), compared with 20.5% of human divisions. The frequency of asymmetric divisions was similar in both species: 23.3% in human and 26.9% in macaque (Fig. 6F). These measurements of the proportion of cell division types directly confirm that, between d38 and d45, human progenitor cells are more likely to proliferate or self renew, whereas macaque progenitor cells undergo neurogenic/terminal pattern of cell divisions.

We conclude that the experimental and theoretical data are consistent with a model for human cortical neurogenesis that proposes an extended period during which progenitor cell expansion is combined with ongoing neurogenesis, reflected in differences in the proliferative behavior of progenitor cells between human and macaque at this stage of development.

Species-specific cortical progenitor cell proliferative behaviour and developmental timing are regulated by cell autonomous mechanisms

Having established that *in vitro*-derived cortical progenitor cells demonstrated species-specific cortical progenitor cell clonal behaviour and clone-size outputs, we tested whether these features of cortical development were cell autonomous or regulated by cell-cell communication. We performed *in vitro*, mixed progenitor cell culture assays between and within species, using single GFP-labeled, d35 human and macaque cortical progenitor cells (Fig. 7A). Mixing GFP-labelled progenitor cells at a 1:100 dilution with their host species, we observed that donor progenitor cells were incorporated into host rosettes readily, indicating that the mechanics of cell adhesion and polarity cues were sufficiently similar to enable efficient co-culture (Fig. 7B).

Transferred progenitor cells proliferated and differentiated to form clones of daughter cells over the subsequent 10-day period (Fig. 7C). Analysing clone size distributions 10 days after setting up mixed cultures, we observed that macaque cortical progenitor cells produced a distribution of clones that tended towards smaller sizes, in which the majority of clones were between two and five cells in size (Fig. 7C). This was similar to the distribution of clones sizes measured by lentiviral labeling of day 40 cultures reported above (Fig. 4). Importantly, the distribution of clone sizes did not differ when GFP-labeled macaque progenitor cells were mixed with unlabeled macaque progenitor cells or mixed with human progenitor cells (Fig. 7C).

The same result was obtained when culturing GFP-labeled human cortical progenitor cells in human or macaque progenitor cell environments (Fig. 7C). Human progenitor cells again demonstrated a species-specific distribution pattern of clone sizes, with a

wider distribution of clone sizes compared with macaque. Again, this finding was similar to the clone size distribution measured by clonal labeling of d40 cultures reported above (Fig. 4). Notably, the wide distribution of clone sizes was unaffected by the species environment, with similar size distributions observed when placed in macaque or human environments (Fig. 7C).

To further explore the contribution of extracellular signaling between progenitor cells, we carried out additional mixing experiments at a lower density of donor cells, culturing GFP-labeled progenitor cells at a dilution of 1:1000 with unlabeled host cells (Fig. 7C). As with the 1:100 experiments, the species environment had no effect on progenitor cell clonal outputs (Fig. 7C). Therefore, we conclude that cortical progenitor cell proliferation, differentiation, and clonal outputs are largely regulated cell autonomously in each species.

During the d35-45 time window, macaque cortical progenitor cells switch from TBR1+ deep layer neurogenesis to the production of SATB2+ upper layer neurons (Fig. 7D). We used the mixed species culture system (1:100 dilution) to investigate whether species' environments could regulate lineage progression, independent of effects on progenitor cell proliferative behaviours.

Clones generated from macaque progenitor cells placed in a macaque background (i.e., macaque to macaque transfers) contained SATB2+ neurons, demonstrating that they underwent species-appropriate developmental switching to produce upper layer/late born

cell types during the 10-day culture period. When placed in a macaque environment during this period, human cortical progenitor cells produced deep layer TBR1+ neurons without producing any upper layer SATB2+ cortical neurons (Fig. 7D, E), continuing to generate the same classes of neurons as they did in their native, human environment. Conversely, when we placed macaque cortical progenitor cells into a human environment to ask whether that environment would suppress lineage progression in the macaque, we found that, under those conditions, macaque progenitor cells proceeded to switch to generate upper layer SATB2+ neurons, whereas the surrounding human host progenitor cells continued to generate TBR1+ deep layer neurons (Fig. 7E).

We further tested the extent to which lineage progression was resistant to environmental cues by co-culturing macaque progenitor cells (1:100 dilution) for 30 days with human or macaque progenitor cells from d25, at which stage both species were initiating production of deep layer, TBR1+ neurons (Fig. 7F). Clonal assignment during longer-term culture was not possible, due to the very large size of the clones generated. However, we could qualitatively assess whether the donor, GFP-expressing cells underwent lineage progression by analyzing whether they produced SATB2+, upper layer neurons. We found that d25 macaque progenitor cells generated equivalent numbers of SATB2+ neurons over the 30-day period, whether in a human or a macaque environment. Together, these data indicate that lineage progression and cell-type specification in each species is controlled by a cell autonomous mechanism, resistant to environmental cues.

DISCUSSION

Using 2D adherent and 3D organoid stem cell systems, we have found that a major determinant of cerebral cortex size in primates is a species-specific program that controls the output of cortical progenitor cells. This program includes a developmental phase in primates that is not prominent in rodents, during which the progenitor cell population is expanding while also generating deep layer, early-born neurons. Most striking is the finding that humans, who have notably larger cerebral cortices that contain more neurons than macaques, have a much longer period during which they balance progenitor cell expansion with neurogenesis. This phase enables the production of larger clones from each founder neuroepithelial cell. The proliferative behaviours of human and macaque cortical progenitor cells, outputting as clone size, and the timing of genesis of different classes of cortical neurons were unaffected by exposure to a different species environment *in vitro*. These data indicate that control of neuronal number and brain size are coordinated in part by a cell autonomous mechanism that is likely to be under genetic control.

Using a range of approaches based on *in vitro* differentiation of PSCs from humans, chimpanzee and two species of macaque in two different cell culture systems, an adherent 2D system (Shi et al., 2012a) and a 3D organoid system (Kadoshima et al., 2013), we have established that species-appropriate timing of major developmental events in cortical development is maintained *in vitro*. These events include the generation of all known cortical progenitor cell types, including oRG cells, from neuroepithelial cells (Florio and Huttner, 2014), the temporal order of genesis of projection neurons (Qian et

al., 1998), the species-appropriate timing of production of different projection neuron types (Workman et al., 2013) and the maturation of the neuronal electrical properties (McCormick and Prince, 1987). These systems allowed us to carry out a series of investigations into the differences in progenitor cell behaviours between human and other primates during cortical development.

Lineage analysis of primate cortical progenitor cells and computational modeling of neurogenesis revealed that primate cortical progenitor cells go through an extended period during which neurogenesis is balanced with expansion of the proliferating progenitor cell population. During rodent corticogenesis, a small proportion of RGCs increase progenitor numbers during neurogenesis (Noctor et al., 2004). However, we found that the length and extent of the progenitor expansion period in primates were markedly longer compared to rodents and differed between humans and macaques: this phase occurred over approximately 30 days in human compared with 15 days in macaque. We experimentally validated the difference in progenitor cell proliferative behaviours between human and macaque at the population and clonal level, including time-lapse imaging of clonal development over 7 days. The consequence of this feature of human cortical development is to increase overall clone size and thus the total number of cortical neuron, which, ultimately, would increase cortical size *in vivo*.

Previous models for the increased size of the human cortex, compared with other primates, have proposed two contributing mechanisms. The radial unit hypothesis for cortical development, when applied to the question of cortical expansion, posits that the

increase in human cortical size is underpinned by an increase in the founder population of neuroepithelial progenitor cells, without major differences in clone size or number of neurons in each radial unit (Geschwind and Rakic, 2013; Rakic, 2000). Alternatively, the increase in cortical size has been proposed to be a result of an increase in the relative numbers of oRGs generated later in development, increasing the numbers of later born, upper layer neurons (Florio and Huttner, 2014; Geschwind and Rakic, 2013).

The extended period of progenitor cell proliferation during the generation of deep layer neurons reported here constitutes another mechanism for increasing cortical size, one that operates during the early stages of neurogenesis to regulate clonal size and composition. This additional mechanism increases the clonal output of progenitor cells in humans, compared with macaque, and would result in a disproportionate increase in the size of human cortex if it occurred to the same extent *in vivo*. Interestingly, this prolonged period of progenitor expansion coincides with the appearance of oRGs in human and macaque cortex *in vivo* (Fietz et al., 2010; Gertz et al., 2014; Hansen et al., 2010). It is possible that the increase in early progenitor cell proliferation in primates may lead to, and include, an expansion of the oRG population. We report here that oRGs are generated during directed differentiation from PSCs of each primate species, as we previously found in human culture systems (Shi et al., 2012a). However, due to the absence of reliable, quantifiable oRG-specific markers, it is not possible currently to definitively address this question in the stem cell systems used here.

The observed differences in progenitor cell output and lineage progression between humans and macaques are largely independent of environmental signals in the stem cell systems used here, and they are most likely regulated by a cell autonomous programme. This finding is consistent with previous studies of primary mouse cortical progenitor cells in culture (Qian et al., 1998; 2000). Studies of the genetic basis for differences in cortical development among different mammals, including primates, have identified a range of genetic differences, including single nucleotide and copy number variants, with differences in the expression and function of copy number variants contributing to several aspects of cortical development (Charrier et al., 2012; Keeney et al., 2014). Differences among mammals in gene use, for example the timing and levels of expression of growth factors and receptors such as PDGF (Lui et al., 2014) and Fzd8 (Boyd et al., 2015) during cortical development, have shown that intercellular signaling is an important regulator of cortical size during *in utero* development. However, differences in intercellular signaling are unlikely to underlie the differences in progenitor cell behavior observed *in vitro*, given the cell-autonomous nature of those behaviors in inter-species, mixed cultures.

In conclusion, we have found that the increase in cortical neuronal number in humans compared with non-human primates, and the subsequent increase in cortical size, is largely determined by differences in cortical progenitor cell outputs. We have identified a feature of primate cortical development whereby cortical progenitor cells expand their population for an extended period during the genesis of deep layer neurons, balancing expansion of the progenitor cell population with neurogenesis. This phase of cortical development does not appear to be prominent in rodents (Gao et al., 2014). As well as

differing between primates and rodents, this aspect of cortical development varies among primates, leading to differences in cortical size between humans and other primates.

Given that this mechanism for controlling cortical size is regulated cell autonomously, *in vitro* stem cell systems of cortical development provide experimental platforms to identify the relevant cellular mechanisms.

EXPERIMENTAL PROCEDURES

Pluripotent stem cell culture and directed cortical differentiation

Human pluripotent stem cells (H9 ESCs, WiCell Research Institute; Edi2 ESCs, from J Nichols, Cambridge (Shi et al., 2012a); NDC1.2 iPSCs (Israel et al., 2012); NAS6 iPSCs, (Devine et al., 2011), chimpanzee iPSCs (chimp 00818 iPSCs and 01029 iPSCs (Marchetto et al., 2013) and macaque ESCs (MF1 ESCs, MF12 ESCs and MN1 ESCs from E. Curnow, Washington National Primate Research Centre) were cultured either with mitomycin-treated mouse embryonic fibroblasts (MEFs) or under feeder-free conditions in Essential 8 Medium on Geltrex-coated tissue culture plates (Life Technologies). Neural induction was performed as previously described (Shi et al., 2012a; 2012b). Following 12 days of induction, the neuroepithelial sheet was broken up using Dispase (Life Technologies), plated onto laminin-coated plates and cultured in N2B27-supplemented medium, including 20ng/ml FGF2 (Peprotech) for 4 days. After day 16 of the induction, cells were maintained in N2B27 medium up to 80 days.

RT-PCR, immunofluorescence and imaging

Total RNA from cortical cultures was isolated using Trizol (Sigma) and reverse-transcribed to cDNA using random hexamer primers (Applied Biosciences). Semi-quantitative RT-PCR was performed using primers against *FOXP1*, *NKX2.1*, *DLX1*, *ISL1*, *CTIP2*, *RORB*, *KCNIP2*, *MDGA1* and *RPS17* and visualized using a Gel Doc XR+ Imager (Biorad). For immunocytochemistry, cells were fixed with 4% paraformaldehyde in PBS and processed for immunofluorescence staining. Primary antibodies used were α -PAX6 (Covance PRB-278P), α -Vimentin (Abcam ab8973), α -phospho-histone H3

(Abcam ab10543), α -atypical PKC (Santa Cruz sc-216), α -Ki67 (BD 550609), α -TBR2 (Abcam ab23345), α -TBR1 (Abcam ab31940), α -MAP2 (Abcam ab10588), α -GFP (Abcam ab4674), α -SATB2 (Abcam ab51502), and α - β III tubulin (Covance PRB-435P). Immunostained samples were imaged using an Olympus FV1000 inverted confocal microscope.

Electrophysiology

For electrophysiological recordings, cortical neurons were incubated with artificial cerebral spinal fluid containing 125mM NaCl, 25mM NaHCO₃, 1.25mM NaH₂PO₄, 3mM KCl, 2mM CaCl₂, 25mM glucose and 3mM pyruvic acid, bubbled with 95% O₂ and 5% CO₂. Borosilicate glass electrodes with resistance of 6-10M Ω were filled with an artificial intracellular solution, containing 135mM potassium gluconate, 7mM NaCl, 10mM HEPES, 2mM Na₂ATP, 0.3mM Na₂GTP and 2mM MgCl₂, and positioned over a cortical neuron to form a whole-cell patch. Recordings were made using a Multiclamp 700A amplifier (Molecular Devices), and signals were sampled and filtered at 20kHz and 6kHz ,respectively. A low-pass Gaussian filter was applied to filter out high frequency noise.

Cortical organoid generation

Cortical organoids were generated as described (Kadoshima et al., 2013). Briefly, human and non-human primate PSCs were dissociated with Accutase (Innovative Cell Technologies), and 12,000 cells were seeded into each well of low-adhesion 96-well plates (Sumitomo Bakelite) in cortical differentiation medium (Glasgow MEM, 20%

knock-out serum replacement, 100 μ M non-essential amino acid, 100 μ M sodium pyruvate, 100 μ M β -mercaptoethanol, 100U/ml penicillin-streptomycin, 3 μ M IWR1e (Millipore) and 5 μ M SB431542). After 18 days, organoids were transferred to a non-adhesive 9-cm petri dish and cultured with post-aggregation medium containing DMEM/F12, N2, chemically defined lipid concentrate (Life Technologies), 0.25mg/ml fungizone (Life Technologies) and 100U/ml penicillin-streptomycin. As the organoids were cultured for longer periods of time, further supplements were added to the post-aggregation medium, including 5 μ g/ml heparin (StemCell Technologies), fetal bovine serum (HyClone), 1% growth factor-reduced Matrigel (BD Biosciences) and B27.

Clonal lineage analysis and interspecies mixed culture assays

Third-generation replication-incompetent lentivirus was produced by calcium phosphate transfection of HEK293T cells, using pBOP-GFP plasmids combined with packaging plasmids pRSV-Rev, pMDLg/pRRE and pMD2.G. For clonal lineage analysis, cortical progenitor cells were plated 3 days before retroviral labeling (at incubation day 20, 30 and 40) at a density of 1.0×10^5 cell/cm³, and infected with the lentivirus at low titres. Cortical cultures were then 'chased' for 2, 6 and 10 days, before being fixed and immunostained. For interspecies mixed culture assays, 'donor' progenitor cells were labeled with high titre lentivirus at day 25 post-induction in two rounds of infection separated by 24 hours. At d35, donor and host cultures were dissociated and mixed in a 1:100 or 1:1000 ratio. Cells were plated at a density of 1.0×10^5 cell/cm³ and incubated for a further 2, 6 and 10 days.

Computational model of cortical progenitor cell neurogenesis

See Supplementary Information 2 for details.

Cell cycle length measurement and BrdU/EdU double labeling

For measuring cell cycle length, 1 μ M EdU was added to the culture medium at day 32 post-neural induction (d32). After 2, 8, 14, 20, 26, 32, 38, 44, 50 further hours in culture, cells were fixed with 4% paraformaldehyde/PBS and EdU incorporation was visualized using the Click-iT imaging kit (Life Technologies). Cell cycle lengths were calculated from cumulative labeling as described (Nowakowski et al., 1989). For BrdU/EdU double labeling, human and macaque cortical progenitor cells/neurons were incubated with 1 μ g/ml BrdU from d40. At d45, BrdU was replaced with 5 μ M EdU, and cells were further cultured for 24 hours. At the end of the EdU labeling period, cells were fixed and stained first for EdU, and then for BrdU using α -BrdU Alexa Flour 488 antibody (MoBU-1: Life Technologies). Immunostained cells were analyzed by flow cytometry (DakoCytomation Cyan ADP MLE Analyser, Beckman Coulter).

Time-lapse imaging of cortical progenitor cells

Replication-incompetent retrovirus was used to label neural progenitors at day 35 post-cortical induction. Following incubation for 72 hours, GFP-labelled neural progenitors were imaged every 12 hours for the following 168 hours. N2B27-supplemented neural culturing medium was replaced with Tyrode's solution, containing low potassium and 2mM CaCl₂, for imaging (Barreto-Chang and Dolmetsch, 2009).

REFERENCES

- Azevedo, F.A.C., Carvalho, L.R.B., Grinberg, L.T., Farfel, J.M., Ferretti, R.E.L., Leite, R.E.P., Jacob Filho, W., Lent, R., and Herculano-Houzel, S. (2009). Equal numbers of neuronal and nonneuronal cells make the human brain an isometrically scaled-up primate brain. *J Comp Neurol* 513, 532–541.
- Barreto-Chang, O.L., and Dolmetsch, R.E. (2009). Calcium imaging of cortical neurons using Fura-2 AM.
- Boyd, J.L., Skove, S.L., Rouanet, J.P., Pilaz, L.-J., Bepler, T., Gordân, R., Wray, G.A., and Silver, D.L. (2015). Human-chimpanzee differences in a FZD8 enhancer alter cell-cycle dynamics in the developing neocortex. *Curr Biol* 25, 772–779.
- Charrier, C., Joshi, K., Coutinho-Budd, J., Kim, J.-E., Lambert, N., de Marchena, J., Jin, W.-L., Vanderhaeghen, P., Ghosh, A., Sassa, T., et al. (2012). Inhibition of SRGAP2 function by its human-specific paralogs induces neoteny during spine maturation. *Cell* 149, 923–935.
- Dehay, C., Kennedy, H., and Kosik, K.S. (2015). The outer subventricular zone and primate-specific cortical complexification. *Neuron* 85, 683–694.
- Devine, M.J., Ryten, M., Vodicka, P., Thomson, A.J., Burdon, T., Houlden, H., Cavaleri, F., Nagano, M., Drummond, N.J., Taanman, J.W., et al. (2011). Parkinson's disease induced pluripotent stem cells with triplication of the alpha-synuclein locus. *Nat Commun* 2, 440.
- Espuny-Camacho, I., Michelsen, K.A., Gall, D., Linaro, D., Hasche, A., Bonnefont, J., Bali, C., Orduz, D., Bilheu, A., Herpoel, A., et al. (2013). Pyramidal neurons derived from human pluripotent stem cells integrate efficiently into mouse brain circuits in vivo. *Neuron* 77, 440–456.
- Fietz, S.A., Kelava, I., Vogt, J., Wilsch-Brauninger, M., Stenzel, D., Fish, J.L., Corbeil, D., Riehn, A., Distler, W., Nitsch, R., et al. (2010). OSVZ progenitors of human and ferret neocortex are epithelial-like and expand by integrin signaling. *Nat Neurosci* 13, 690–699.
- Florio, M., and Huttner, W.B. (2014). Neural progenitors, neurogenesis and the evolution of the neocortex. *Development* 141, 2182–2194.
- Gao, P., Postiglione, M.P., Krieger, T.G., Hernandez, L., Wang, C., Han, Z., Streicher, C., Papisheva, E., Insolera, R., Chugh, K., et al. (2014). Deterministic progenitor behavior and unitary production of neurons in the neocortex. *Cell* 159, 775–788.
- Gertz, C.C., Lui, J.H., LaMonica, B.E., Wang, X., and Kriegstein, A.R. (2014). Diverse behaviors of outer radial glia in developing ferret and human cortex. *Journal of Neuroscience* 34, 2559–2570.

- Geschwind, D.H., and Rakic, P. (2013). Cortical evolution: judge the brain by its cover. *Neuron* 80, 633–647.
- Hansen, D.V., Lui, J.H., Parker, P.R., and Kriegstein, A.R. (2010). Neurogenic radial glia in the outer subventricular zone of human neocortex. *Nature* 464, 554–561.
- Herculano-Houzel, S. (2009). The human brain in numbers: a linearly scaled-up primate brain. *Front Hum Neurosci* 3, 31.
- Herculano-Houzel, S. (2012). The remarkable, yet not extraordinary, human brain as a scaled-up primate brain and its associated cost. *Proceedings of the National Academy of Sciences* 109 Suppl 1, 10661–10668.
- Herculano-Houzel, S., Collins, C.E., Wong, P., and Kaas, J.H. (2007). Cellular scaling rules for primate brains. *Proc Natl Acad Sci U S A* 104, 3562–3567.
- Israel, M.A., Yuan, S.H., Bardy, C., Reyna, S.M., Mu, Y., Herrera, C., Hefferan, M.P., Van Gorp, S., Nazor, K.L., Boscolo, F.S., et al. (2012). Probing sporadic and familial Alzheimer's disease using induced pluripotent stem cells. *Nature* 482, 216–220.
- Kadoshima, T., Sakaguchi, H., Nakano, T., Soen, M., Ando, S., Eiraku, M., and Sasai, Y. (2013). Self-organization of axial polarity, inside-out layer pattern, and species-specific progenitor dynamics in human ES cell-derived neocortex. *Proceedings of the National Academy of Sciences* 110, 20284–20289.
- Keeney, J.G., Davis, J.M., Siegenthaler, J., Post, M.D., Nielsen, B.S., Hopkins, W.D., and Sikela, J.M. (2014). DUF1220 protein domains drive proliferation in human neural stem cells and are associated with increased cortical volume in anthropoid primates. *Brain Struct Funct*.
- Kirwan, P., Turner-Bridger, B., Peter, M., Momoh, A., Arambepola, D., Robinson, H.P.C., and Livesey, F.J. (2015). Development and function of human cerebral cortex neural networks from pluripotent stem cells in vitro. *Development* 142, 3178–3187.
- Kornack, D.R., and Rakic, P. (1995). Radial and horizontal deployment of clonally related cells in the primate neocortex: relationship to distinct mitotic lineages. *Neuron* 15, 311–321.
- LaMonica, B.E., Lui, J.H., Wang, X., and Kriegstein, A.R. (2012). OSVZ progenitors in the human cortex: an updated perspective on neurodevelopmental disease. *Curr. Opin. Neurobiol.* 22, 747–753.
- Lui, J.H., Nowakowski, T.J., Pollen, A.A., Javaherian, A., Kriegstein, A.R., and Oldham, M.C. (2014). Radial glia require PDGFD-PDGFR β signalling in human but not mouse neocortex. *Nature* 515, 264–268.
- Marchetto, M.C.N., Narvaiza, I., Denli, A.M., Benner, C., Lazzarini, T.A., Nathanson, J.L., Paquola, A.C.M., Desai, K.N., Herai, R.H., Weitzman, M.D., et al. (2013).

Differential L1 regulation in pluripotent stem cells of humans and apes. *Nature* 503, 525–529.

Mariani, J., Simonini, M.V., Palejev, D., Tomasini, L., Coppola, G., Szekely, A.M., Horvath, T.L., and Vaccarino, F.M. (2012). Modeling human cortical development in vitro using induced pluripotent stem cells. *Proceedings of the National Academy of Sciences* 109, 12770–12775.

McConnell, S.K. (1988). Development and decision-making in the mammalian cerebral cortex. *Brain Research Reviews* 13, 1–23.

McConnell, S.K. (1992). The control of neuronal identity in the developing cerebral cortex. *Curr. Opin. Neurobiol.* 2, 23–27.

McCormick, D.A., and Prince, D.A. (1987). Post-natal development of electrophysiological properties of rat cerebral cortical pyramidal neurones. *The Journal of Physiology* 393, 743–762.

Molyneaux, B.J., Arlotta, P., Menezes, J.R.L., and Macklis, J.D. (2007). Neuronal subtype specification in the cerebral cortex. *Nat Rev Neurosci* 8, 427–437.

Mountcastle, V.B., Mountcastle, V.B., and Mountcastle, V.B. (1998). *The Cerebral Cortex* (Cambridge, Mass.: Harvard University Press).

Noctor, S.C., Martinez-Cerdeno, V., Ivic, L., and Kriegstein, A.R. (2004). Cortical neurons arise in symmetric and asymmetric division zones and migrate through specific phases. *Nat Neurosci* 7, 136–144.

Nowakowski, R.S., Lewin, S.B., and Miller, M.W. (1989). Bromodeoxyuridine immunohistochemical determination of the lengths of the cell cycle and the DNA-synthetic phase for an anatomically defined population. *Journal of Neurocytology* 18, 311–318.

Ostrem, B.E.L., Lui, J.H., Gertz, C.C., and Kriegstein, A.R. (2014). Control of outer radial glial stem cell mitosis in the human brain. *Cell Rep* 8, 656–664.

Qian, X., Goderie, S.K., Shen, Q., Stern, J.H., and Temple, S. (1998). Intrinsic programs of patterned cell lineages in isolated vertebrate CNS ventricular zone cells. *Development* (Cambridge, England) 125, 3143–3152.

Qian, X., Shen, Q., Goderie, S.K., He, W., Capela, A., Davis, A.A., and Temple, S. (2000). Timing of CNS cell generation: a programmed sequence of neuron and glial cell production from isolated murine cortical stem cells. *Neuron* 28, 69–80.

Rakic, P. (2000). Radial unit hypothesis of neocortical expansion. *Novartis Found Symp* 228, 30–42; discussion42–discussion52.

Shi, Y., Kirwan, P., Smith, J., Robinson, H.P., and Livesey, F.J. (2012a). Human cerebral

cortex development from pluripotent stem cells to functional excitatory synapses. *Nat Neurosci* 15, 477–486.

Shi, Y., Kirwan, P., and Livesey, F.J. (2012b). Directed differentiation of human pluripotent stem cells to cerebral cortex neurons and neural networks. *Nature Protocols* 7, 1836–1846.

Smart, I.H.M., Dehay, C., Giroud, P., Berland, M., and Kennedy, H. (2002). Unique morphological features of the proliferative zones and postmitotic compartments of the neural epithelium giving rise to striate and extrastriate cortex in the monkey. *Cereb Cortex* 12, 37–53.

Walsh, C., and Cepko, C.L. (1988). Clonally related cortical cells show several migration patterns. *Science* 241, 1342–1345.

Workman, A.D., Charvet, C.J., Clancy, B., Darlington, R.B., and Finlay, B.L. (2013). Modeling transformations of neurodevelopmental sequences across mammalian species. *Journal of Neuroscience* 33, 7368–7383.

AUTHOR CONTRIBUTIONS

T.O. and F.J.L. designed the study, T.O. conducted the experiments, B.S. carried out the lineage analysis and computational modelling, C.M. and F.G. generated chimpanzee iPSCs, and all authors wrote the paper.

ACKNOWLEDGEMENTS

The authors thank Ayiba Momoh for technical assistance, Prof. Yoshiki Sasai for training in organoid culture methods, and Eliza Curnow (Washington) for the provision of macaque embryonic stem cells. TO was supported by the Wellcome Trust PhD Programme in Developmental Biology at the University of Cambridge. FJL and BDS are Wellcome Trust Investigators. This research was supported by core funding to the Gurdon Institute by the Wellcome Trust and Cancer Research UK. FHG was supported by The Helmsley, Mathers and JPB Foundations.

FIGURE LEGENDS

Figure 1: Replication of species-appropriate developmental timing of cortical neurogenesis *in vitro* from PSCs of multiple primate species

- A.** Schematic comparing the *in vivo* developing cortical neuroepithelium and *in vitro*, stem cell-derived cortical neuroepithelial rosette. In a cortical rosette, the aPKC⁺ apical surface is at the rosette centre, immediately surrounded by the ventricular zone (VZ)-like region containing PAX6/Vimentin⁺ radial glial progenitor cells (RGPs). Outside the VZ, there is no clear positional distinction between inner subventricular zone (iSVZ) and outer SVZ (oSVZ), where both TBR2⁺ intermediate progenitor cells (IPCs) and PAX6/Vimentin⁺ outer RGP-like cells are found. These progenitor cells produce cortical neurons (such as TBR1/MAP2⁺ thalamic projection neurons), which then migrate away from the rosette centre.
- B.** Representative immunofluorescence images of cortical neuroepithelial rosettes derived from human (HS1, HS2, HS3 and HS4), chimpanzee (PT1 and PT2) and macaque (MF1, MF2 and MN1) PSCs. Antibodies used are as indicated: PAX6/Vimentin (RGPs), aPKC (apical cell domain), TBR2/Ki67 (IPs) or TBR1/MAP2 (layer VI cortical neurons). Scale bars, 50µm.
- C.** Semi-quantitative RT-PCR for the cortically expressed transcription factor (TF), *FOXP1*, and ventrally/caudally expressed TFs, *NKX2.1*, *DLX1* and *ISL1*. All cortical progenitor cells from human and non-human primate PSCs are dorsal pallial in regional identity, unless treated with the Smoothened/Hedgehog agonist

- purmorphamine (HS1+Pur.) during induction to ventralise the progenitor cells to non-cortical identities.
- D.** The cerebral cortex is organized into 6 layers of excitatory projection neurons with defined gene expression profiles, based on detailed studies of the mouse cerebral cortex (Molyneaux et al., 2007): thalamic projection neurons in layer VI express TBR1, subcerebral projection neurons in layer V express CTIP2, and callosal projection neurons in layer II-IV express RORB, SATB2, KCNIP2 and MDGA1.
- E.** Immunofluorescence images of *in vitro*-derived cortical neurons of human, chimpanzee and macaque at the indicated development stages post-cortical induction (d30 to d70). Cultures were stained for TBR1 and SATB2 to monitor differentiation of deep and upper layer neurons (yellow arrowheads indicate first SATB2⁺ neurons generated). Scale bars, 200µm.
- F.** Quantification of the relative proportions of TBR1⁺ and SATB2⁺ neurons in human (HS1 and HS2), chimpanzee (PT2) and macaque (MF1, MF2 and MN1) cultures at the indicated developmental stages (d30 to d70).
- G.** Semi-quantitative RT-PCR of expression of *CTIP2* (layer V), *RORB* (layer IV), *KCNIP2* and *MDGA1* (Layer II-IV) at the indicated stages in human, chimpanzee and macaque cortical cultures. Transcripts enriched in later-born, upper layer neurons (*RORB*, *KCNIP2*, *MDGA1*) are expressed at an earlier stage in macaque than in humans or chimpanzee.

Figure 2: Timing of cortical neurogenesis is independent of neuronal lamination and three-dimensional organisation

- A. Chimpanzee cerebral cortex organoids (scale bar, 200 μ m). Organoids develop *in vivo*-like organization of ventricular zone (VZ), with PAX6+/Ki67+ polarized (apical aPKC localization) progenitor cells within the VZ, apical mitoses (pH3+ cells) and IPCs at the outer margin of the VZ. Antibodies as indicated in each panel. Scale bar, 100 μ m
- B. Human, chimpanzee and macaque cortical organoids undergo sequential production of TBR1⁺ deep layer neurons and SATB2⁺ upper layer neurons (yellow arrowheads indicate initial SATB2⁺ neurons generated). As organoids developed for longer periods, cortical neurons migrated to form cortical plate-like structures (yellow bracket) with some separation of layers of TBR1⁺ and SATB2⁺ neurons. Scale bars, 50 μ m.
- C. Scatter plots of positions of TBR1⁺ and SATB2⁺ neurons relative to the ventricular surface in human d80, chimpanzee d80 and macaque d60 cortical organoids. Red lines represent median positions.

Figure 3: Functional maturation of primate neurons demonstrates species-specific timing

- A. Detection of miniature excitatory post-synaptic currents (mEPSCs) in whole cell recordings of human (HS2), chimpanzee (PT1) and macaque (MF2) cortical neurons. Spontaneous depolarisations indicate the presence of synaptic activity.

B. Patch-clamp, single neuron recordings of electrophysiological properties of cortical neurons at different developmental stages (d30-70) for human (HS1 and HS2), chimpanzee (PT1) and macaque (MF1, MF2 and MN1). In response to stepwise current stimulation (-10 to 20pA), *in vitro* cortical neurons fired action potentials (APs). The response to current injection evolved over time, with mature neurons firing more APs following single stimuli. Numbers represent frequencies of patterns of AP firing at each given developmental stage.

Figure 4: Clonal analysis reveals marked differences between human and macaque cortical progenitor cell dynamics over developmental time

- A. Single cortical progenitor cells were labeled with low titre, replication-incompetent lentiviruses at clonal resolution (see Supplementary Information 1 for further details). Following infection at d20, d30, or d40, progenitor cells were cultured for 2, 6 or 10 days, fixed and immunostained for analysis.
- B. Representative immunofluorescence images of clones derived from a single progenitor cell after 2, 6 or 10 day-chase periods (panels as labeled), immunostained for Ki67 (cycling progenitor cells) and β III-tubulin (post-mitotic neurons). Scale bar, 100 μ m.
- C. Human and macaque clone size distributions for each developmental stage (d20, d30 and d40), at each time point post-labeling (2, 6 and 10 days). Red horizontal bars represent medians and vertical bars indicate the interval between the first and third quartiles of the clonal distribution. Data for each species are combined from four human pluripotent cell lines (2 ESCs, 2 iPSCs) and from three macaque ESC

lines. Total number of clones analysed for each line: HS1, n=440; HS2, n=43; HS3, n=201; HS4, n= 93; MF1, n=247; MF2, n=469; MN1, n=303.

D. Human and macaque average clone sizes for time points shown in C. Significant differences between the average sizes of human and macaque clones at d30+10 ($p = 0.0437$), d40+6 ($p = 0.0154$) and d40+10 ($p = 0.205 \times 10^{-2}$) are labeled. Error bars, s.d.

Figure 5: Differences in clone growth between macaque and human are reflected by differences in progenitor cell proliferative behaviours

- A. Quantification of the average number of Ki67⁺ progenitors in a human or macaque clone after various chase periods (2, 6 and 10 days) following clonal labeling at d20, d30 and d40. Data analysis for this and subsequent panels are from two human lines (HS1, HS3) and three macaque lines (MF1, MF2 and MN3). Error bars represent s.d.
- B. Average size of all ‘persisting’ clones (which contain one or more Ki67⁺ progenitor cells) with different chase periods following clonal labeling at d20, 30 and d40. The black solid line represents the theoretically predicted values for persisting clone expansion following d40 labeling (See Supplementary Information 2 for further details on the computational model). Error bars, s.d.
- C. Percentage of human and macaque ‘exited’ clones (which no longer contain any Ki67⁺ progenitor cells) with different chase periods after clonal labeling at d20, d30 and 40. Error bars, s.d.

D. Human and macaque clone size distributions of total and persisting clones after clonal labeling at d40 and analysis 2, 6 and 10 days after labeling. Red dotted lines represent theoretically predicted values (see Supplementary Information 2 for details of computational modeling).

Figure 6: Testing predictions of progenitor cell proliferative behaviours during human and macaque cortical development

- A. Experimental design of BrdU/EdU double-labeling assay. From d40, BrdU was added to human and macaque cortical cultures to cumulatively label all progenitor cells and their progeny until d45, at which point BrdU was switched to EdU to reveal the ratio of persisting progenitor cells (BrdU⁺EdU⁺) to exited progenitor cells (BrdU⁺EdU⁻).
- B. Representative scatterplot of EdU/BrdU double-labeling assay analyzed by flow cytometry. Three distinct populations of cells are evident: BrdU⁻EdU⁻ non-cycling cells (which were post-mitotic at the beginning of the experiment), BrdU⁺EdU⁻ exited progenitor cells and BrdU⁺EdU⁺ persisting progenitor cells. The proportion of progenitor cells persisting after 5 day-chase (BrdU⁺EdU⁺/all BrdU⁺) is higher for human than macaque (p=0.0119). Human data average of n=4; macaque data average of n=5. Error bars, s.d.
- C. Time-lapse imaging of human and macaque cortical progenitor cell divisions. GFP-labelled progenitors in clones were followed and imaged every 12 hours

- over a period of 168 hours. From the sequential images, a lineage tree of clonal progenitor divisions was reconstructed. Cells were assigned as ‘progenitor’ if they divided in the span of recording (red circle), ‘post-mitotic’ if they did not divide for more than 60 hours (equivalent to the third quartile of the distribution of all cell divisions recorded) (blue circle), or ‘unknown/apoptotic’ if cells either disappeared from the imaging frame or were born close to the end of filming period (grey circle).
- D. Representative lineage trees showing cell divisions of human (HS1 and HS2) and macaque (MF1 and MF2) progenitors, re-constructed from sequential images.
 - E. Bar graphs showing distributions of the lengths of cell cycles based on reconstructed lineage trees for human (blue) and macaque progenitor cells (orange).
 - F. Pie-charts showing proportions of cell division types for human and macaque progenitors, based on reconstructed lineage trees. ‘Proliferative’ divisions are those giving rise to two progenitors, ‘Asymmetric’ divisions giving one progenitor and one post-mitotic cells, and ‘Terminal’ division giving two post-mitotic cells.

Figure 7: Species-specific cortical progenitor cell proliferative behaviour and developmental timing are regulated by cell autonomous mechanisms

- A. Schematic representation of the experimental design of *in vitro* inter-species mixed culture assays. Cortical progenitor cells of species A were labeled with cytoplasmic GFP, delivered by high titre lentivirus, and subsequently mixed with GFP⁻ progenitors from species B in a 1:100 or 1:1000 ratio at post-cortical

- induction day 35 (d35). Transplanted cortical progenitor cells were cultured with host cells for 2, 6 and 10 days (d35+2, d35+6 and d35+10) before being fixed and immunostained.
- B. Immunofluorescence images of GFP⁺ human and macaque clones, introduced into macaque and human backgrounds, respectively. GFP⁺ cortical progenitor cells were efficiently incorporated into rosettes of host species (white dotted line). Scale bars, 50µm.
- C. The size distributions of human HS1 clones and macaque MF2 clones in either human or macaque backgrounds at d35+10. Red horizontal lines indicate median clone sizes and vertical lines show the span between 25% and 75% quartiles for each distribution. N = number of clones analysed for each culture condition. Dilution of donor cells to host cells (1/100, 1/1000) are as shown.
- D. Representative immunofluorescence images of GFP⁺ human (HS1) or macaque (MF2) clones introduced into macaque background. Cultures were immunostained for transcription factors expressed by deep (TBR1) and upper (SATB2) cortical neurons. Yellow arrowheads indicate SATB2⁺ upper layer neurons produced from a transplanted macaque progenitor cell. Scale bars, 100µm.
- E. Proportions of TBR1⁺ and SATB2⁺ cortical neurons generated by transplanted progenitor cells of each species in each background as indicated. Host/recipient environment does not affect cell types generated by each species. N = number of cells expressing each transcription factor.

F. Representative immunofluorescence images showing a long-term chimeric mixture of human (HS1) and macaque (MF2) neural progenitors. Single macaque progenitors were introduced into a human (HS1) or macaque (MF2) background at d25. The mixed cultures were incubated further for 30 days, and fixed and stained for the presence of upper layer cortical neurons (SATB2+: yellow arrowheads). Scale bars, 150 μ m.

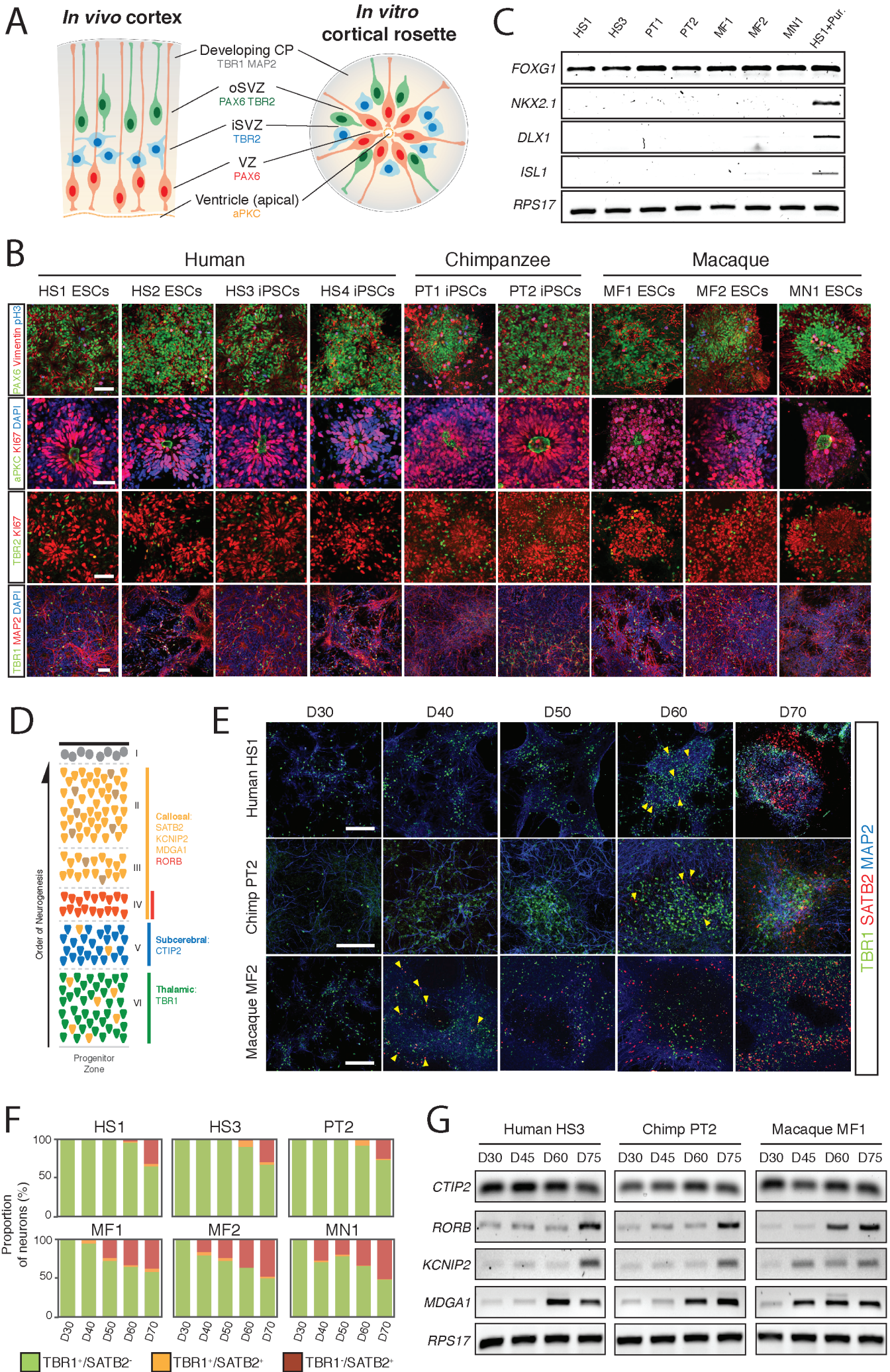


Figure 1

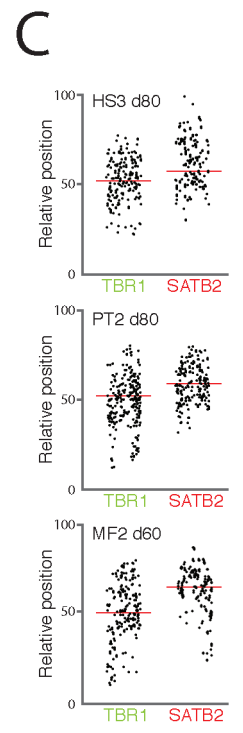
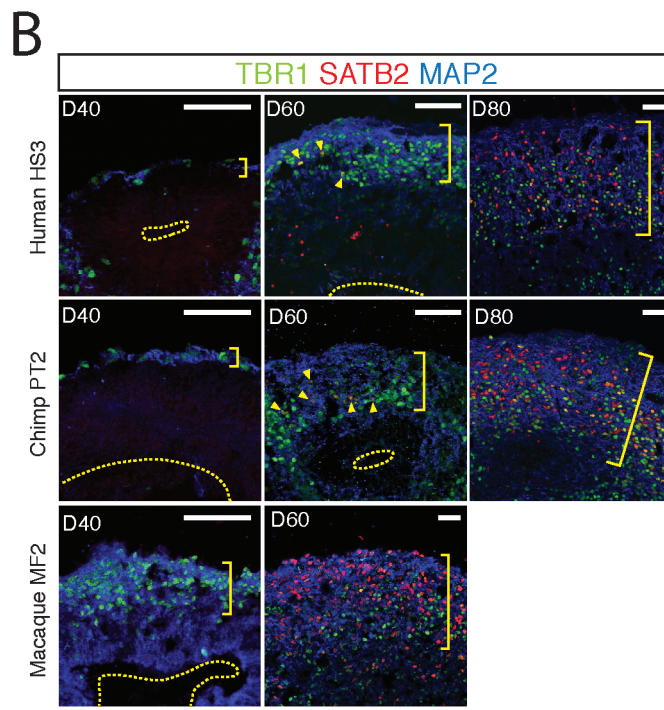
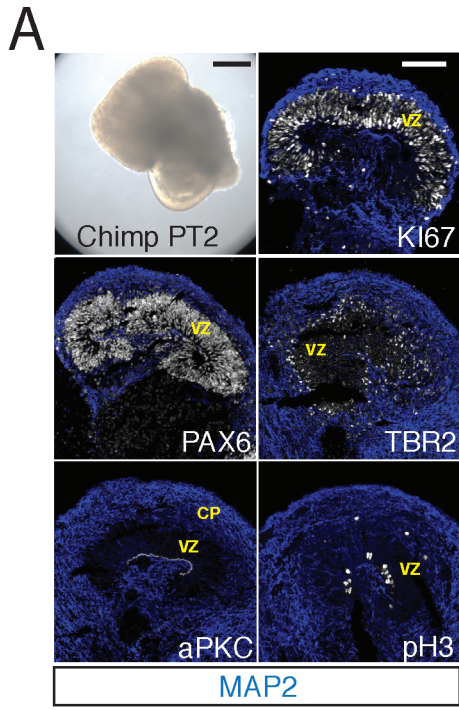


Figure 2

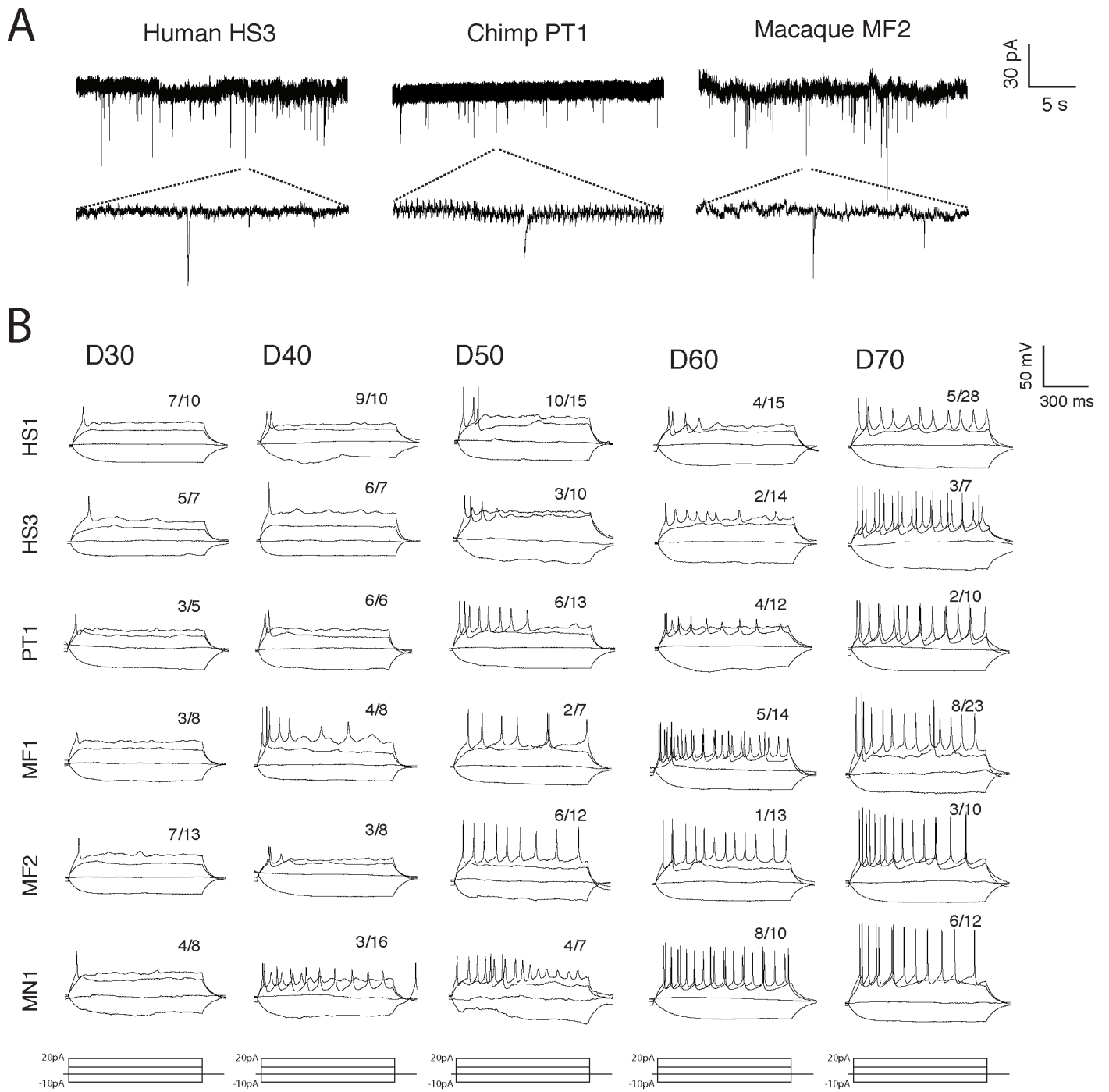


Figure 3

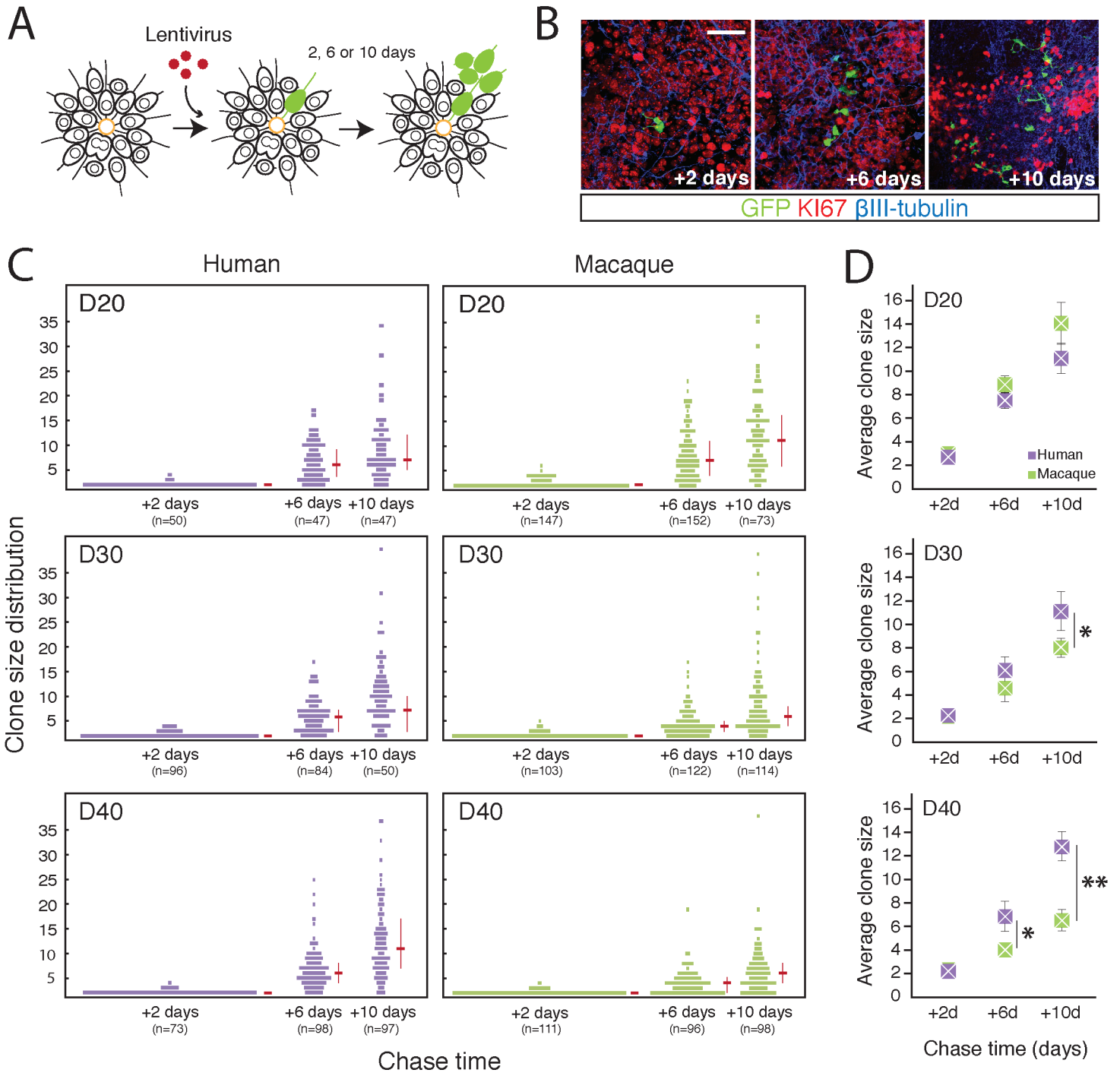


Figure 4

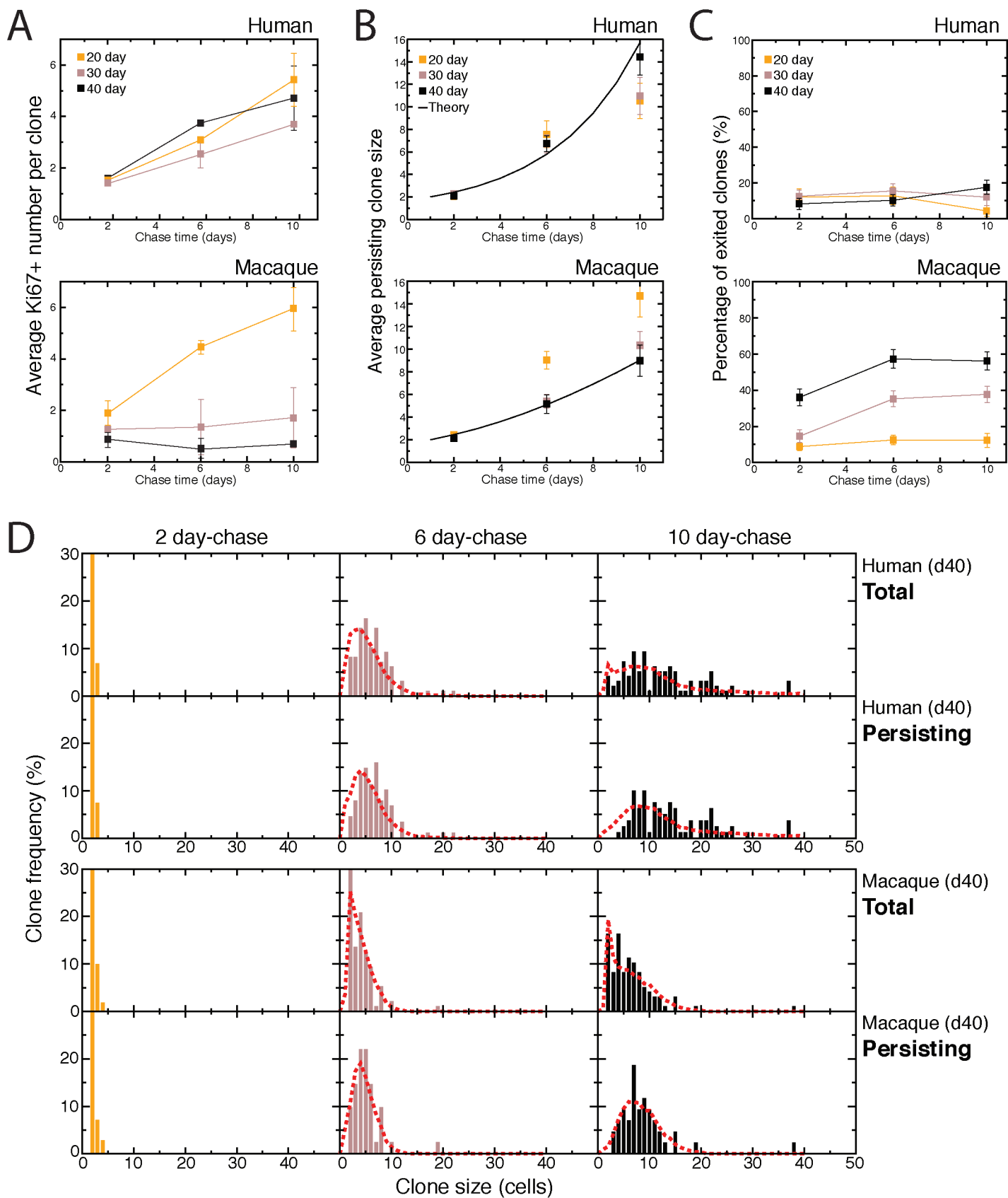


Figure 5

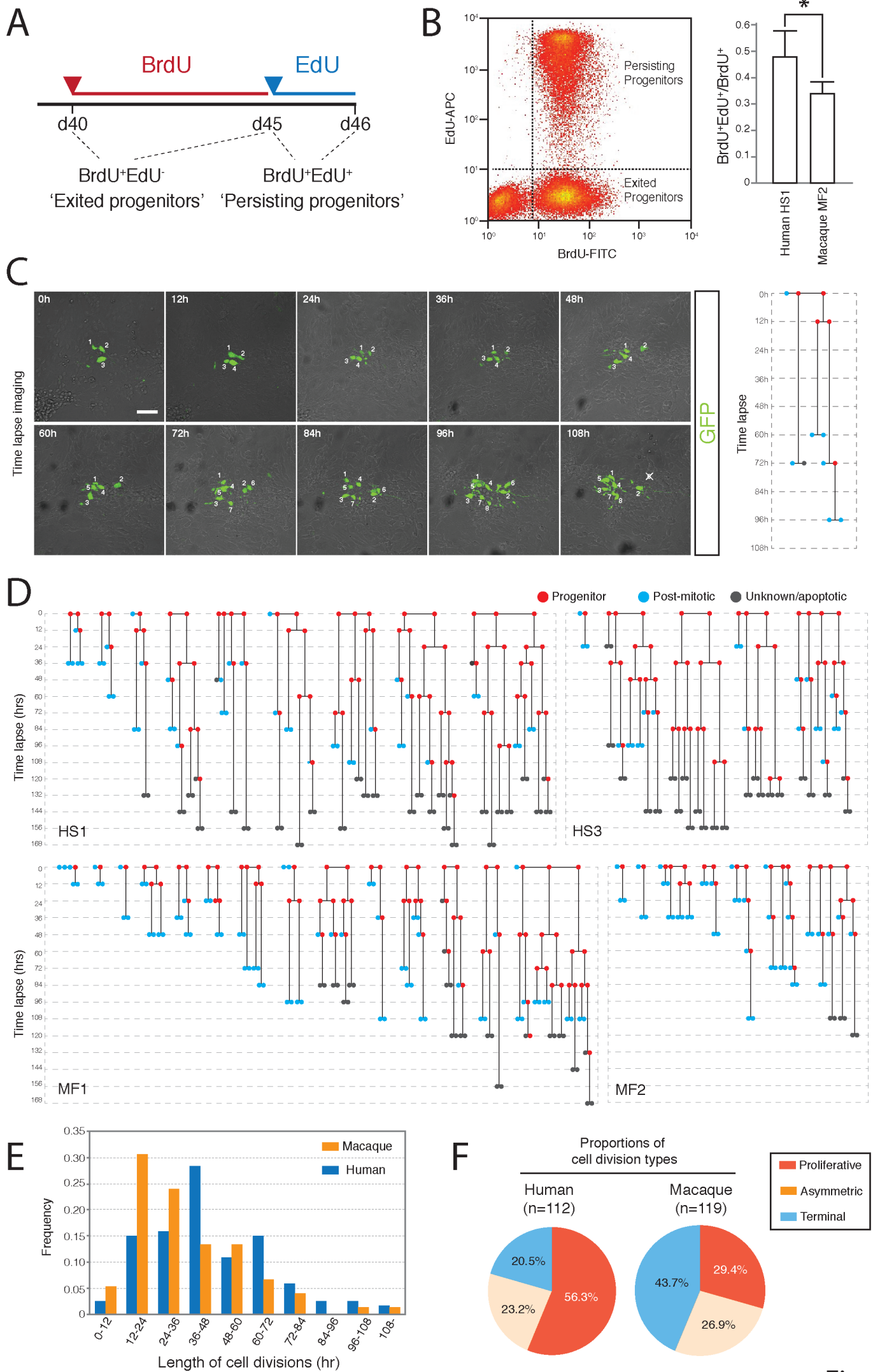


Figure 6

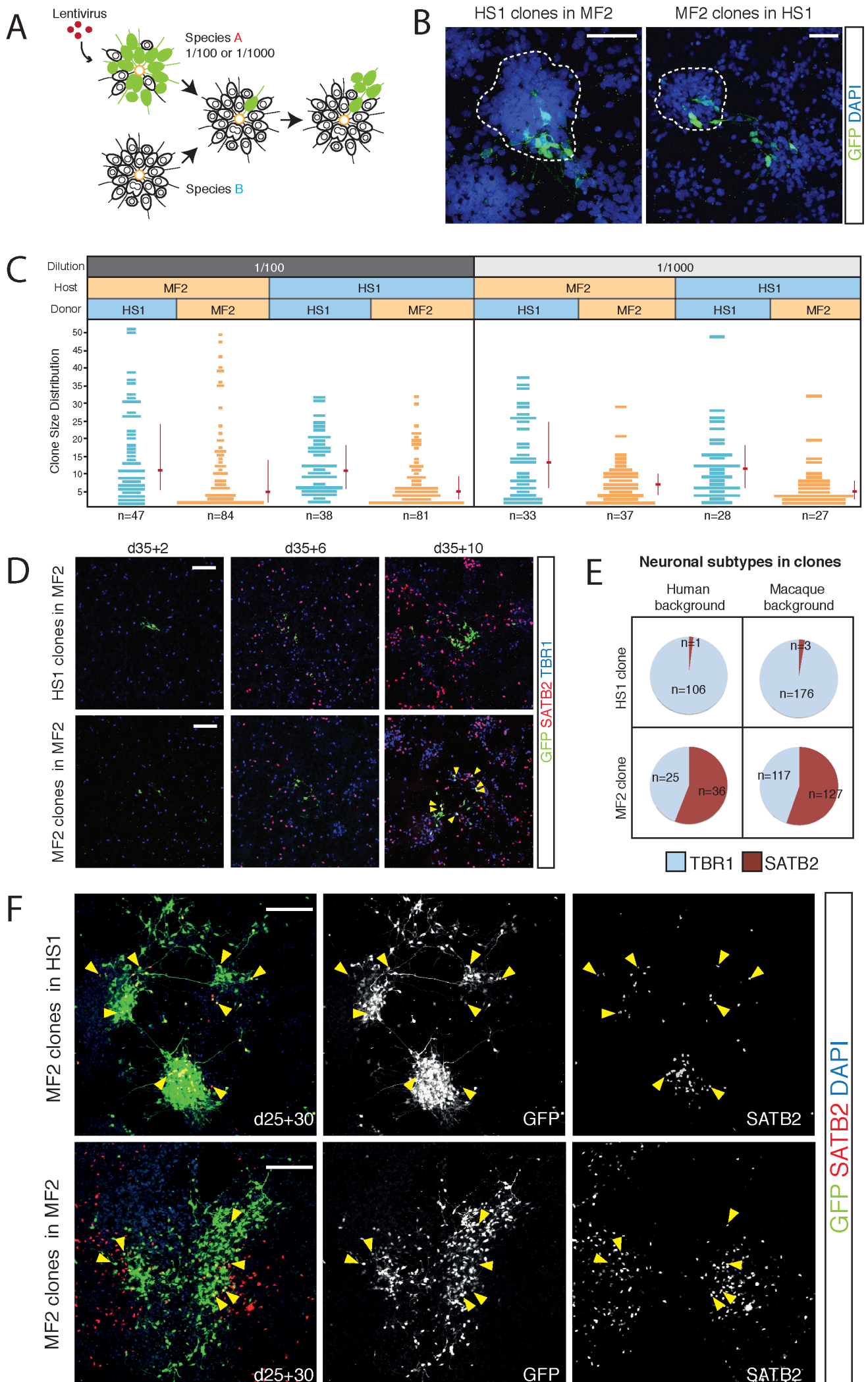


Figure 7